Direct extraction of equivalent circuit parameters for on-chip spiral transformers*

Wei Jiaju(韦家驹), Wang Zhigong(王志功)†, and Li Zhiqun(李智群)

Institute of RF- & OE-ICs, Southeast University, Nanjing 210096, China

Abstract: This paper compares model differences of transformers measured in 4-port and 2-port configurations. Although 2-port configuration is more appropriate for measurement and application, it brings tremendous difficulties to the model's parameter extraction. In this paper, a physics-based equivalent circuit model and its corresponding direct extraction procedure are proposed for on-chip transformers. The extraction is based on the measurement of 2-port configuration instead of the 4-port type, and it can capture the model parameters without any optimization. In this procedure, a new method has been developed for the parameter extraction of the ladder circuit, which is commonly used to represent the skin effect. Thus, this method can be transferred to the modeling of other passive devices, such as on-chip transmission lines, inductors, baluns, etc. In order to verify the procedure's efficiency and accuracy, an on-chip interleaved transformer in a 90 nm 1P9M CMOS process has been fabricated. We compare the modeled and measured self-inductance, the quality factor, mutual reactive and resistive coupling coefficients. Excellent agreement has been found over a broad frequency range.

Key words: transformer; model; extraction; equivalent circuit; ladder; skin effect
DOI: 10.1088/1674-4926/33/1/015012 **EEACC:** 2570

1. Introduction

On-chip spiral transformers are valuable passive components in radio-frequency integrated circuits (RFICs), such as voltage-controlled oscillators, power amplifiers, and low-noise amplifiers. To represent the electrical performance of on-chip transformers for circuit simulations and optimizations, a compact equivalent circuit model is much more convenient than an electromagnetic field solver (e.g., HFSS or momentum). How to obtain the model parameters is always a concern for modeling engineers and circuit designers.

In recent years, some physics-based modeling methods to calculate the model parameters from the transformer geometry and process parameters have been developed[1−8]. However, the process parameters are not always well defined for modeling purposes. In addition, some expressions are merely empirical formulas which depend on a specific fabrication process. Since most of the physics-based modeling may only provide certain estimates, numerical optimization is often used to achieve a high accuracy. Unfortunately, numerical optimization takes a long time and yields multiple solutions. Also, the non-optimal solution may not comply with scaling rules because of its non-physical meaning.

Compared with the modeling methods discussed above, direct extraction is more suitable for modeling because it can achieve a high accuracy and have a reasonable physical meaning. To model on-chip transformers, the extraction methods differed enormously depending on the configuration types in the measurement. Actually, the transformer can be measured in the 4-port (Fig. 1(a) in Ref. [9]) and 2-port (Fig. 1 in Ref. [2]) configurations, and their equivalent circuit models are simply illustrated in Fig. 1. In the 4-port configuration, we can easily extract the series and shunt branches of one coil by setting the other coil open[9]. However, it is not convenient to measure a 4-port device by using a 2-port vector network analyzer (VNA), and applications of the transformer often adopt the 2-port configuration (two terminals are connected to ground or virtual ground). In the 2-port configuration, we can find that the inductive series branch and conductive shunt branch have mixed together to make the extraction very difficult. To the best of the author's knowledge, the investigations into the extraction of the model parameters for the transformer in 2-port configuration are really scarce.

This paper proposes a direct extraction procedure to capture the parameters of the 2-port transformer model, and it can achieve a high accuracy over a broad frequency range without any optimization.

2. Equivalent circuit model

As shown in Fig. 2(b), a physics-based equivalent circuit model is proposed to model on-chip spiral transformers. In this model, the sub-network consisting of R_{si}, L_{si}, R_{pi} and L_{pi} (i = 1, 2) is used to account for the skin effect of each coil. C_{subi} and R_{subi} represent the characteristics of the conductive silicon substrate. C_{oxi} models the oxide-layer capacitance between the metal and the substrate. R_{oi} is introduced to account for the spiral coil's conductor loss originated from a lossy substrate return path[10]. C_{oi} denotes the underpass capacitance. The magnetic and electric couplings between two coils are represented by M and C_p, respectively.

3. Direct parameter extraction procedure

3.1. Model transformation

Since the fabricated transformer layout (Fig. 2(a)) is de-

* Project supported by the Yangzi–Delta Cooperative Projects of Zhejiang Province, China.
† Corresponding author. Email: zgwang@seu.edu.cn
Received 10 July 2011, revised manuscript received 4 August 2011

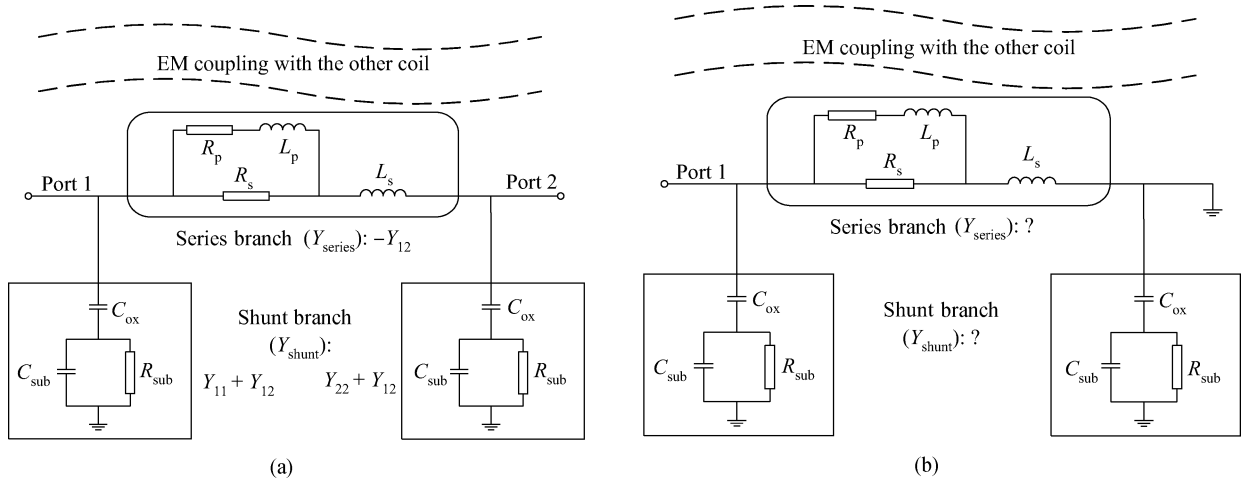

Fig. 1. Half of transformer model in (a) 4-port and (b) 2-port configurations.

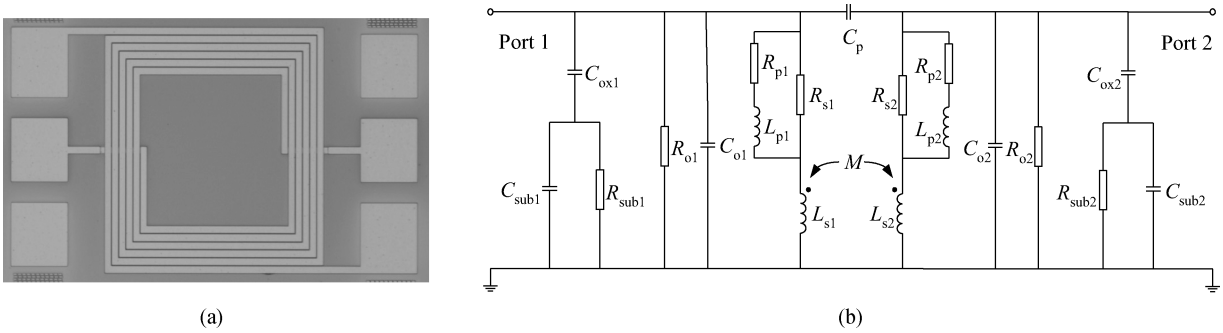

Fig. 2. (a) Top view of a fabricated on-chip transformer and (b) its equivalent circuit model.

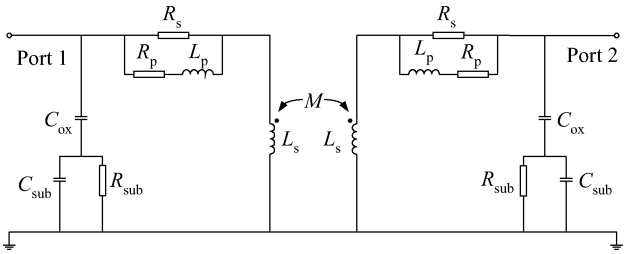

Fig. 3. Simplified model.

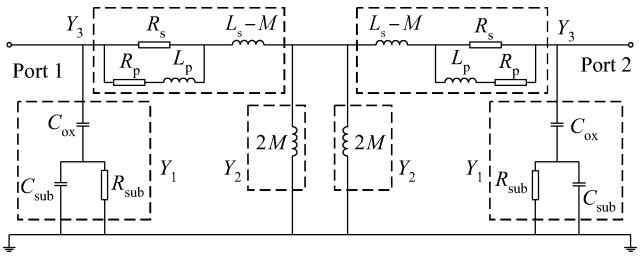

Fig. 4. Model with two back-to-back cascading Π cells.

signed symmetrically, the model can be simplified to a symmetrical network and the index "*i*" is omitted from the element denotation for simplicity. According to the data in Ref. [9], C_p and C_o in Fig. 2(b) are relatively small. And R_o generally shows a very large value with the substrate resistivity of about 10 Ω·cm from our experience. Thus, these elements can be temporarily neglected when the frequency is not very high. Then, we can get the simplified model, as shown in Fig. 3.

After decoupling and some other simple transformation steps, we can get the 2-port topology with two back-to-back cascading Π cells in Fig. 4.

3.2. Separation of the shunt and series branches

In Fig. 4, the S-matrix of the entire device is designated as $[S^m] = \begin{pmatrix} S_{11} & S_{12} \\ S_{21} & S_{22} \end{pmatrix}$ and the values of the matrix can be obtained from the 2-port measurement. Meanwhile, $[T^m] = \begin{pmatrix} A & B \\ C & D \end{pmatrix}$ represents the *ABCD*-matrix of the entire device. $[T_1] = \begin{pmatrix} a & b \\ c & d \end{pmatrix}$ and $[T_2] = \begin{pmatrix} d & b \\ c & a \end{pmatrix}$ denote the *ABCD*-matrices of the two back-to-back cascading Π cells, respectively. According to the conversions between 2-port network parameters, we can get

$$A = \frac{(1+S_{11})(1-S_{22})+S_{12}S_{21}}{2S_{21}}, \tag{1}$$

$$B = Z_0\frac{(1+S_{11})(1+S_{22})-S_{12}S_{21}}{2S_{21}}, \tag{2}$$

$$C = \frac{(1-S_{11})(1-S_{22})-S_{12}S_{21}}{2Z_0S_{21}}, \tag{3}$$

$$D = \frac{(1-S_{11})(1+S_{22})+S_{12}S_{21}}{2S_{21}}, \tag{4}$$

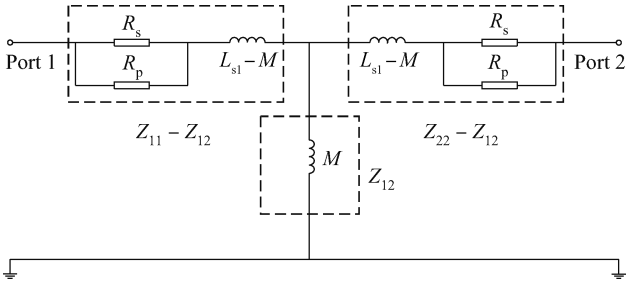

Fig. 5. Simplified T-topology at the low frequencies.

where Z_0 denotes the characteristic impedance of the testing ports.

As shown in Fig. 4, the admittances of the dashed boxes are denoted by Y_1, Y_2 and Y_3. It can be seen that Y_1 is the admittance of the shunt branch, while the combination of Y_2 and Y_3 includes the information of the series branch. Thus, in order to separate the shunt and series branches in the model, we should get the values of Y_1, Y_2 and Y_3 with the aid of known parameters (e.g. $[S^m]$ and $[T^m]$). According to the definition of the *ABCD*-matrix, we can get

$$a = 1 + Y_2/Y_3, \tag{5}$$

$$b = 1/Y_3, \tag{6}$$

$$c = Y_1 + Y_2 + Y_1 Y_2/Y_3, \tag{7}$$

$$d = 1 + Y_1/Y_3. \tag{8}$$

The *ABCD*-matrix of the 2-port network equals the product of two cascading cell's *ABCD*-matrices, we get

$$\begin{pmatrix} A & B \\ C & D \end{pmatrix} = \begin{pmatrix} a & b \\ c & d \end{pmatrix} \times \begin{pmatrix} d & b \\ c & a \end{pmatrix}. \tag{9}$$

Substituting Eqs. (5)–(8) into Eq. (9), we have

$$A = \frac{2Y_1(Y_2+Y_3) + Y_3(2Y_2+Y_3)}{Y_3^2}, \tag{10}$$

$$B = \frac{2(Y_2+Y_3)}{Y_3^2}, \tag{11}$$

$$C = \frac{2(Y_1+Y_3)(Y_1Y_2+Y_2Y_3+Y_3Y_1)}{Y_3^2}, \tag{12}$$

$$D = \frac{2Y_1(Y_2+Y_3) + Y_3(2Y_2+Y_3)}{Y_3^2}. \tag{13}$$

From Eqs. (10)–(13), we get

$$Y_1 = (A - \sqrt{1+2BY_2})/B, \tag{14}$$

$$Y_3 = (1 + \sqrt{1+2BY_2})/B. \tag{15}$$

At low frequencies, the model in Fig. 3 can be further simplified. As shown in Fig. 5, the simplified model demonstrates itself as a standard T-topology when the frequency is approaching DC, and the impedances of the dashed boxes are also provided using the Z-parameters of the 2-port network.

Thus, M can be determined as

$$M = \text{imag}(Z_{12})/\omega\,|_{\omega\to 0}. \tag{16}$$

Then, the admittance Y_2 in Fig. 4 can be determined as

$$Y_2 = 0.5/\text{j}\omega M. \tag{17}$$

3.3. Extraction for the shunt branch

The shunt branch is composed of three elements, i.e., C_{ox}, C_{sub} and R_{sub}. Using the real part and imaginary part of the admittance (i.e., Y_1), Reference [11] introduced two useful characteristic functions as

$$f_1(\omega) = \frac{\omega^2}{\text{real}(Y_1)}, \tag{18}$$

$$f_2(\omega) = \frac{\text{imag}(Y_1)}{\text{real}(Y_1)}\omega. \tag{19}$$

In this paper, we directly use the method developed in Ref. [11] to extract the values of C_{ox}, C_{sub} and R_{sub}, and the detailed process is omitted.

3.4. Extraction for the series branch

The series branch consisting of R_s, $L_s - M$, R_p and L_p forms a ladder circuit. The real part and imaginary part of the ladder's impedance (i.e., $Z_s = 1/Y_3$) can be written as

$$\text{rz} = \text{real}(Z_s) = \frac{R_s(R_sR_p + R_p^2 + L_p^2\omega^2)}{(R_s+R_p)^2 + L_p^2\omega^2}, \tag{20}$$

$$\text{lz} = \frac{\text{imag}(Z_s)}{\omega} = (L_s - M) + \frac{L_pR_s^2}{(R_s+R_p)^2 + L_p^2\omega^2}. \tag{21}$$

Combining Eq. (20) and Eq. (21) properly, we developed two new characteristic functions as

$$\begin{aligned} f_3 &= \frac{\omega^2 - \omega_0^2}{(\text{lz}/\text{rz}) - (\text{lz}/\text{rz})_{\omega\to\omega_0}} \\ &= -\frac{(R_sR_p + R_p^2 + L_p^2\omega^2)(R_sR_p + R_p^2 + L_p^2\omega_0^2)}{L_p^2[L_pR_s + (L_s-M)(R_s+R_p)]} \\ &= p_1 + p_2\omega^2, \end{aligned} \tag{22}$$

$$\begin{aligned} f_4 &= \frac{(\omega^2 - \omega_0^2)(\text{lz} - \text{lz}_{\omega\to\omega_0})}{\text{rz} - \text{rz}_{\omega\to\omega_0}} \\ &= -\frac{L_p(\omega^2 - \omega_0^2)}{R_s + R_p} = q_1 + q_2\omega^2, \end{aligned} \tag{23}$$

where ω_0 is the reference frequency for the characteristic functions. It can be chosen arbitrarily in the development of f_3 and f_4, but from our experience, these characteristic functions show a better linearity when ω_0 is relatively low. Thus, ω_0 has been set as the minimum frequency of the measurement in our extraction process.

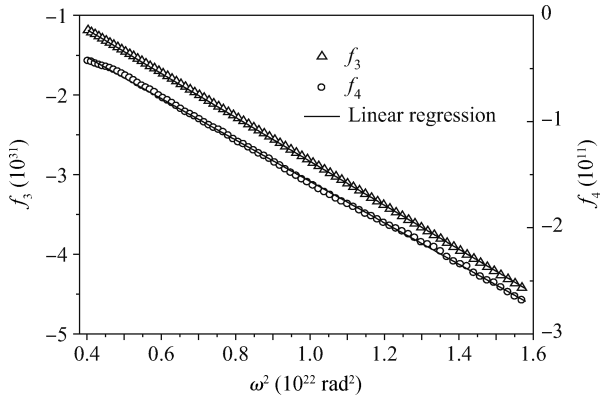

Fig. 6. f_3 and f_4 as a function of ω^2 based on measurement.

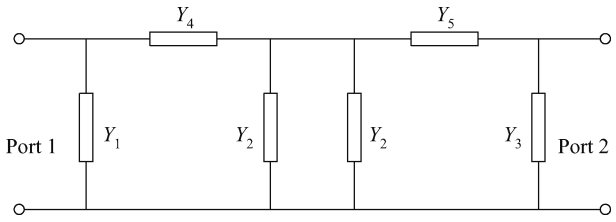

Fig. 7. Simple illustration of asymmetrical transformers.

Demonstrated in Fig. 6, f_3 and f_4 exhibit a good linear dependence on ω^2. Thus, p_1, p_2, q_1 and q_2 can be extracted by linear regression easily. Then, we can get

$$k = p_2/(p_1 q_2^2) - 1, \tag{24}$$

$$R_\mathrm{p} = \mathrm{rz}_{\omega\to 0}(1 + 1/k), \tag{25}$$

$$R_\mathrm{s} = R_\mathrm{p} k, \tag{26}$$

$$L_\mathrm{p} = (R_\mathrm{s} + R_\mathrm{p})(-q_2), \tag{27}$$

$$L_\mathrm{s} = \mathrm{lz}_{\omega\to\omega_0} - L_\mathrm{p} R_\mathrm{s}^2 / \left[(R_\mathrm{s} + R_\mathrm{p})^2 + L_\mathrm{p}^2 \omega_0^2\right] + M. \tag{28}$$

It should be emphasized here that the ladder circuit is commonly used to represent the skin effect in the modeling of many passive components, such as on-chip transmission lines, inductors, baluns, etc. In the literature much effort has been made to extract the ladder's parameters. In Ref. [12], the constant resistance ratio and inductance ratio are estimated for round wires by empirical formulas, and Reference [11] obtains the ladder's parameters based on iterations. By contrast, the method proposed in this paper (i.e., Eqs. (20)–(28)) can extract the parameters of the ladder circuit without any optimization and it will also not be confined to specific structures.

3.5. Extraction for R_o, C_o and C_p

In Fig. 2(b), we can get the 2-port Y-parameters $[Y^s]$ by simulation with R_o, C_o and C_p neglected and other elements set with values extracted from above steps. $[Y^m]$ denotes the 2-port Y-parameters converted from the measured S-parameters. Then, R_o, C_o and C_p can be extracted at the resonant frequency as

$$C_\mathrm{o} = \mathrm{imag}(Y_{11}^m + Y_{12}^m - Y_{11}^s - Y_{12}^s)/\omega, \tag{29}$$

$$R_\mathrm{o} = 1/\mathrm{real}(Y_{11}^m + Y_{12}^m - Y_{11}^s - Y_{12}^s), \tag{30}$$

$$C_\mathrm{p} = \mathrm{imag}(Y_{12}^s - Y_{12}^m)/\omega. \tag{31}$$

3.6. Extraction procedure for asymmetrical transformers

We can extend the application of our extraction procedure to asymmetrical transformers. In view of the device's asymmetry, the symmetrical topology of Fig. 4 has been modified to form an asymmetrical network. Illustrated in Fig. 7, Y_1 and Y_3 are the admittances of the two coils' shunt branches, while the combination of Y_2 and Y_4 (or Y_2 and Y_5) includes the information of the coil's series branch. Following the similar extraction step in Section 3.2, we can get

$$Y_1 = \frac{A + Dk - \sqrt{A^2 - 2ADk + k(4 + D^2 k + 8BY_2)}}{2Bk}, \tag{32}$$

$$Y_3 = kY_1, \tag{33}$$

$$\begin{aligned} Y_4 = {} & \Big\{(2 - A + Dk)Y_2 \\ & + \sqrt{Y_2^2\,[A^2 - 2ADk + k(4 + D^2 k + 8BY_2)]}\Big\} \\ & \times [-1 + A + k - Dk + 2BkY_2]^{-1}, \end{aligned} \tag{34}$$

$$\begin{aligned} Y_5 = {} & \Big\{[A - (-2 + D)k]Y_2 \\ & + \sqrt{Y_2^2\,[A^2 - 2ADk + k(4 + D^2 k) + 8BkY_2]}\Big\} \\ & \times (1 - A - k + Dk + 2BY_2)^{-1}, \end{aligned} \tag{35}$$

where Y_2 can be determined by Eqs. (16) and (17). The introduced factor k represents the ratio of two shunt branches' admittances, and it can be set as the length ratio of two coils by neglecting the fringing effect. By setting $k = 1$ and $D = A$, we can get the results for symmetrical transformers, i.e. Eqs. (14) and (15). Following the same steps in Sections 3.3–3.5, all the parameters of the asymmetrical transformers can be extracted with ease.

4. Experimental verification and discussion

As shown in Fig. 2(a), an on-chip interleaved transformer has been fabricated in a 90 nm 1P9M CMOS process with substrate resistivity of about 10 Ω·cm and top metal thickness of 3 μm. The line width and line spacing are 8 and 1.5 μm, respectively, and the outer diameter of the transformer is 291 μm.

Table 1. Extracted model parameters for the transformer.

$R_{s1}(R_{s2})$ $R_{p1}(R_{p2})$ (Ω)	$L_{s1}(L_{s2})$ $L_{p1}(L_{p2})$ (nH)	R_{sub1} (R_{sub2}) $R_{o1}(R_{o2})$ (Ω)	M (nH)	C_{ox1} (C_{ox2}) C_{sub1} (C_{sub2}) (fF)	$C_{o1}(C_{o2})$ C_p (fF)
20.93	3.69	186.6	3.214	49.17	6
2.59	0.47	7400		33.12	5

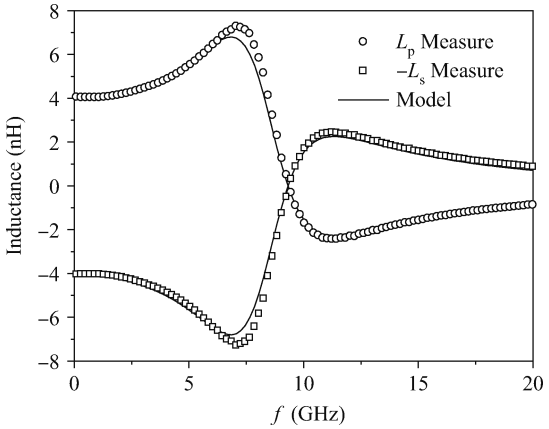

Fig. 8. Self-inductance (L_p and L_s) comparison.

2-port S-parameters were measured and the pad parasitics were de-embedded from the measurement using the open pad structure. Then, after the direct extraction procedure, the model parameters are extracted and listed in Table 1.

We use Z-parameters converted from the measured S-parameters to extract the self-inductance (L_p and L_s), quality factors (Q_p and Q_s), and mutual reactive and resistive coupling coefficients (k_{im} and k_{re}) as functions of frequency. These parameters are calculated using the following expressions:

$$L_p = \frac{\mathrm{Im}(Z_{11})}{2\pi f}, \tag{36}$$

$$L_s = \frac{\mathrm{Im}(Z_{22})}{2\pi f}, \tag{37}$$

$$Q_p = \frac{\mathrm{Im}(Z_{11})}{\mathrm{Re}(Z_{11})}, \tag{38}$$

$$Q_s = \frac{\mathrm{Im}(Z_{22})}{\mathrm{Re}(Z_{22})}, \tag{39}$$

$$k_{im} = \sqrt{\frac{\mathrm{Im}(Z_{12})\mathrm{Im}(Z_{21})}{\mathrm{Im}(Z_{11})\mathrm{Im}(Z_{22})}}, \tag{40}$$

$$k_{re} = \sqrt{\frac{\mathrm{Re}(Z_{12})\mathrm{Re}(Z_{21})}{\mathrm{Re}(Z_{11})\mathrm{Re}(Z_{22})}}. \tag{41}$$

In order to verify the procedure's efficiency and accuracy, we have compared the modeled and measured L_s, L_p, Q_p, Q_s, k_{im} and k_{re}. In Figs. 8 and 9, we compared the curves of $-L_s$ and $-Q_s$ instead of L_s and Q_s for the figures' clearness, respectively. As demonstrated in these two figures, an excellent agreement has been found over a broad frequency band. In

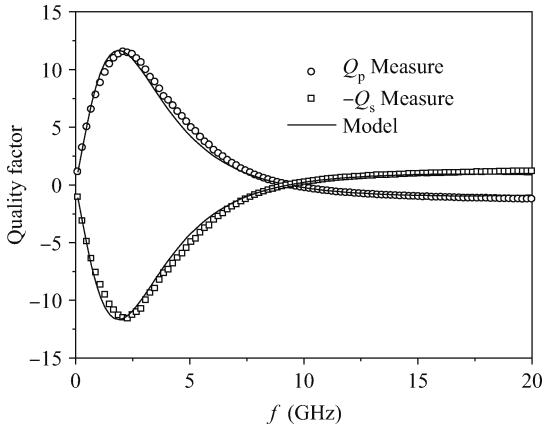

Fig. 9. Quality factor (Q_p and Q_s) comparison.

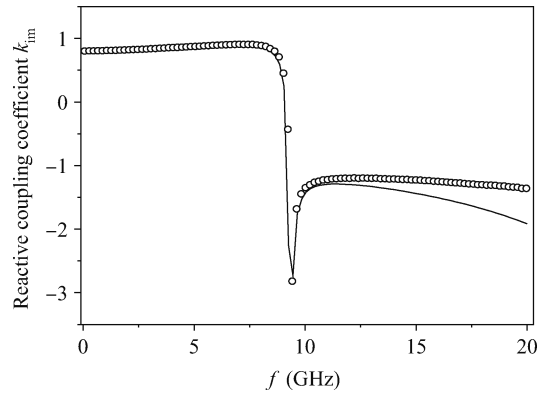

Fig. 10. Reactive coupling coefficient (k_{im}) comparison.

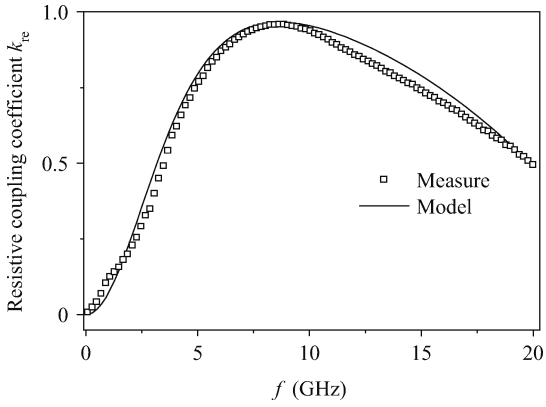

Fig. 11. Resistive coupling coefficient (k_{re}) comparison.

Figs. 10 and 11 we note that the curves of k_{im} and k_{re} agree well below 10 GHz while they exhibit some deviations at higher frequencies. It may be due to the fact that the transformer model in Fig. 2(b) cannot include all effects of the device especially at the high frequencies. Some effects, e.g. the eddy current loss in silicon, have a small influence on the device performance at low frequencies. But these effects will be more apparent when the frequency is high. Taking all effects into account will make the transformer model more complex and bring tremendous difficulties to the parameter extraction procedure. Fortunately, the deviations appear at the frequencies much higher than the

transformer's resonant frequency. In addition, the magnitude of the deviations is very small. Hence, the model in Fig. 2(b) is accurate enough to model the transformer over a broad frequency range and the proposed direct extraction procedure shows its high efficiency and accuracy without any optimization.

5. Conclusion

A direct extraction procedure for on-chip interleaved transformers has been proposed. The extraction is based on the measurement of 2-port configuration, and it can capture the model parameters without any optimization. An excellent agreement between the simulation and measurement over a broad frequency range has demonstrated the procedure's efficiency and accuracy.

References

[1] Gharniti O E, Kerherve E, Begueret J B. Modeling and characterization of on-chip transformers for silicon RFIC. IEEE Trans Microw Theory Tech, 2007, 55(4): 607

[2] Lin L, Yin W, Mao J, et al. Performance characterization of circular silicon transformers. IEEE Trans Magnetics, 2008, 44(12): 4684

[3] Wang C, Liao H, Xiong Y, et al. A physics-based equivalent-circuit model for on-chip symmetric transformers with accurate substrate modeling. IEEE Trans Microw Theory Tech, 2009, 57(4): 980

[4] Gao W, Jiao C, Liu T, et al. Scalable compact circuit model for differential spiral transformers in CMOS RFICs. IEEE Trans Electron Devices, 2006, 53(9): 2187

[5] Long J R. Monolithic transformers for silicon RF IC design. IEEE J Solid-State Circuits, 2000, 35(9): 1368

[6] Tsui C, Tong K Y. Modeling of multilayer on-chip transformers. IEE Proceedings on Microwaves, Antennas and Propagation, 2006, 153: 483

[7] Gharniti O, Kerherve E, Begueret J, et al. Modeling of integrated monolithic transformers for silicon RF IC. IEEE International Conference on Electronics, Circuits and Systems, 2004

[8] Mohan S S, Yue C P, Wong S S, et al. Modeling and characterization of on-chip transformers. International Electron Devices Meeting, 1998

[9] Liao H, Wang C. A new approach to parameter extraction for on-chip symmetric transformers. IEEE International Symposium on Radio-Frequency Integrated Technology, 2009

[10] Guo J C, Tan T Y. A broadband and scalable model for on-chip inductors incorporating substrate and conductor loss effects. IEEE Trans Electron Devices, 2006, 53(3): 413

[11] Huang F, Lu J, Zhang X, et al. Frequency independent asymmetric double-equivalent circuit for on-chip spiral inductors: physics-based modeling and parameter extraction. IEEE J Solid-State Circuits, 2006, 41(10): 2272

[12] Kim S, Neikirk D P. Compact equivalent circuit model for the skin effect. IEEE MTT-S International Microwave Symposium Digest, 1996